Structure of Sodium Glycodeoxycholate Micellar Aggregates from Small-Angle X-ray Scattering and Light-Scattering Techniques

Sara Cozzolino,[†] Luciano Galantini,[†,‡] Edoardo Giglio,[†] Sven Hoffmann,[§] Claudia Leggio,[†,‡] and Nicolae Viorel Pavel*[,†,‡]

Dipartimento di Chimica and Research Center SOFT-INFM-CNR, Università di Roma "La Sapienza", P.le A. Moro 5, 00185 Roma, Italy, and Dubble CRG/ESRF, c/o BP 220 F38043, France

Received: February 2, 2006; In Final Form: April 28, 2006

Ⓦ **This paper contains enhanced objects available on the Internet at http://pubs.acs.org/jpcbfk.**

Small-angle X-ray scattering (SAXS) and dynamic light scattering (DLS) measurements were accomplished on sodium glycodeoxycholate (NaGDC) aqueous electrolyte solutions as a function of NaGDC and NaCl concentrations with the aim to determine with satisfactory approximation the NaGDC micellar aggregate structure at a gross molecular level, assuming monodispersity. Different conditions of interparticle interactions by varying ionic strength (NaCl concentration from 0 to 0.70 M) and NaGDC concentration (from 0.02 to 0.10 M) were studied. Smeared scattering intensities and electron pair distance distribution functions, radii of gyration, and aggregate heights are in satisfactory agreement with the corresponding functions calculated using a 2_1 helix as model. It is formed by trimers, each one composed by three NaGDC and nine H_2O molecules related by a 3-fold rotation axis, and can be described by a hollow cylinder, probably filled by water molecules, characterized by a conventional radius of 23.7 Å and a trimer repeat along the helical axis of 3.6 Å. The helix is considerably inhomogeneous since the volume of the cylinder occupied by NaGDC molecules is less than one-third of the total. On the other hand, calculations performed with the average radial electronic density of the helix without water molecules or totally filled by water molecules (a NaGDC/H_2O molecular ratio of about 1/50) or by using a three-shell average radial electronic density, independently evaluated on absolute scale, do not show significant differences, thus supporting the helical model. The aggregate size increases for all the samples by increasing either the NaCl or NaGDC concentration. The NaGDC low concentration (0.02 M) samples with NaCl within the range 0.30−0.70 M are characterized by short cylindrical aggregates that do not give rise to sensible interference effects. This assertion is supported by the satisfactory fit between the observed apparent mean hydrodynamic radii and the calculated ones by means of the method of Ortega and Garcia de la Torre (*J. Chem. Phys.* **2003**, *119*, 9914), valid for rods with a length-to-diameter ratio ≥0.1 in dilute solution (noninteracting rods). The NaGDC moderate concentration (0.10 M) samples with NaCl within the range 0.20−0.60 M are characterized by cylindrical aggregates that, in the presence of repulsive Coulombic interactions progressively more and more screened, produce interference effects, due to the hard-body repulsion and attractive forces, but the agreement between observed and calculated SAXS data is satisfactory. The results of the low and moderate NaGDC concentration samples seem to indicate that the aggregation number increase, produced by adding 0.10 M NaCl, is constant within an ionic strength range and occurs by the addition of oligomers formed by trimers. The samples with a variable NaGDC concentration (0.02−0.10 M) at a fixed and high NaCl concentration (0.6 M) contain cylindrical aggregates that give rise to an attractive term effect prevailing on the hard-body repulsive one. The same situation seems to occur in the NaGDC moderate concentration samples.

Introduction

The determination of physical and chemical parameters of the bile salt micellar aggregates is a subject of considerable biological and medical importance mainly because they are natural systems. This paper deals with small-angle X-ray scattering (SAXS) and dynamic light scattering (DLS) studies of the sodium salt of 3α,12α-dihydroxy-5β-cholanoylglycine (sodium glycodeoxycholate, NaGDC, Figure 1) with the aim

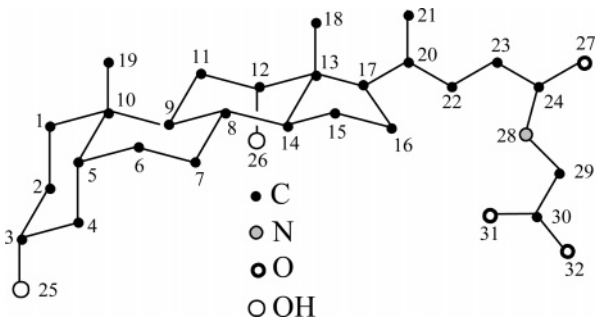

Figure 1. Molecular formula and atomic numbering of the glycodeoxycholate anion. Hydrogen atoms are omitted.

* Corresponding author. Telephone: (+39)-06-49913652. Fax: (+39)-06-490631. E-mail: v.pavel@caspur.it.
[†] Dipartimento di Chimica, Università di Roma "La Sapienza".
[‡] Research center SOFT-INFM-CNR, Università di Roma "La Sapienza".
[§] Dubble CRG/ESRF.

10.1021/jp060712x CCC: $33.50
Published on Web 06/03/2006

to evaluate typical micellar parameters characterizing the structure, size, and shape of NaGDC micellar aggregates.

Previously, two articles concerning NaGDC aqueous electrolyte solutions appeared in the literature. The first one deals with static light scattering and DLS measurements as a function of NaGDC and NaCl concentration (within the range 0.018−0.059 M and 0.03−0.2 M, respectively) and temperature (within the range 20−35 °C).[1] The apparent molar mass and diffusion coefficient as well as the mean aggregation number and hydrodynamic radius of the micellar aggregates were derived, and the interaction potential between two micellar aggregates was estimated in agreement with the Derjaguin−Landau−Verwey−Overbeek (DLVO) theory.[2] The second one deals with SAXS and DLS measurements.[3] The NaGDC concentration was 0.10 M and that of NaCl was within the range 0−0.40 M for SAXS measurements, while the NaGDC and NaCl concentration ranges were 0.02−0.10 M and 0−0.40 M, respectively, for DLS measurements. A comparison of SAXS and DLS measurements pointed out that the Coulombic repulsion prevails at low ionic strength and decreases by adding NaCl. The van der Waals attraction effect predominates at NaCl concentrations greater than about 0.20 M. By assuming very simple models in the treatment of SAXS and DLS data, a fair agreement was generally obtained between the hydrodynamic radii and the geometrical parameters of the SAXS fits.

Furthermore, other recent X-ray studies indicated that the sodium salt of 3α,12α-dihydroxy-5β-cholanoyltaurine (sodium taurodeoxycholate, NaTDC) forms similar cylindrical aggregates in concentrated aqueous solution (40.0 wt %) and in fibers.[4,5] The NaTDC aggregates in solution are 2_1 or pseudo 2_1 helices having as the repetitive unit a trimer constituted by three NaTDC molecules related by a 3-fold rotation axis coinciding with the helical axis. The 2_1 helix is generated by only one rotation angle of 60° of the trimer, whereas the pseudo 2_1 helix has two rotation angles, the sum of which is 120°. The trimer repeat (*t*) along the helical axis is 3.6 Å, and its radius (*r*) is 15.8_5 Å.[5]

The *r* value represents the distance of the most protruding non-hydrogen atom (the oxygen O_{25} at 3α position) from the aggregate helical axis (which coincides with the trimer rotation axis) and has been taken by convention as the helical radius. An oxygen atom of the carboxylate group (O_{32}) is the closest one to the helical axis.

On the other hand, NaGDC and NaTDC fiber structures are very similar,[4] NaGDC and NaTDC aqueous solutions behave similarly,[6−8] and, therefore, NaGDC and NaTDC micellar aggregate structures should be very similar.[8] This hypothesis is also strongly supported by electromotive force measurements carried out as a function of ionic strength, pH, and bile salt concentration.[9,10] NaTDC micellar aggregation numbers are generally multiples of three,[9] while both NaTDC and NaGDC aqueous electrolyte solutions contain trimers, even at the highest ionic strengths,[9,10] in accordance with the helical model formed by trimers. Moreover, the study of aqueous solutions containing both NaGDC and NaTDC together with 0.80 M NaCl to minimize charge interactions showed that the two bile salts form two-component aggregates in which the NaGDC and NaTDC trimers seem to be interchangeable to some extent.[8]

However, the NaTDC helical geometry changes in passing from solid to liquid phases. The *t* and *r* values are, respectively, 6.4 and 10.2 Å in the fiber,[4] 3.6 and 15.8_5 Å in a concentrated aqueous solution (40.0 wt %),[5] and 3.6 and ∼25 Å in dilute aqueous solutions.[7,8] The *r* values indicate that the trimer path from the fiber to the isotropic solution phase resembles the opening of an umbrella and that the opening increases when the NaTDC concentration decreases in solution.[5] A similar behavior is to be expected in the case of NaGDC. Preliminary SAXS results of a 0.10 M NaGDC aqueous solution containing 0.70 M NaCl confirmed this reasonable assumption and showed that the *t* and *r* values, which are, respectively, 6.4 and 10.1 Å in the NaGDC fiber,[4] could be 3.6 and 21.7 Å for this sample.[8]

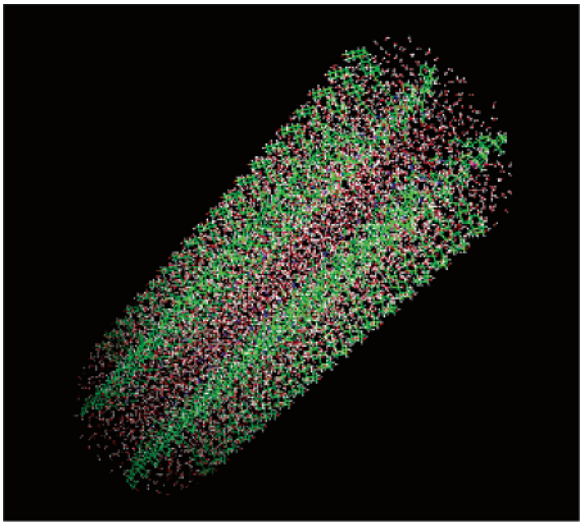

Figure 2. View of the NaGDC model (39 trimers) used in this work. The green lines and red dots represent NaGDC molecules and the oxygen atoms of water molecules, respectively. This drawing has been built using PyMOL. PyMOL is a trademark of DeLano Scientific LLC.

Ⓦ A 3D rotatable image of the hydrated model in PDB format is available.

In this paper, a trimer is formed by 3NaGDC + $9H_2O$. The best available NaGDC anion geometry was assumed, namely that observed in the sodium glycocholate crystal structure,[11] with a side chain nearly fully extended. The axis passing through O_{25} and O_{32} (Figure 1) makes an angle of 85° with the trimer rotation axis in the best model inferred from SAXS experimental data (for the atomic coordinates, see the Supporting Information). Hydrated sodium ions are tentatively but reasonably located near the carboxylate and amide groups and constitute the glue holding together two anions of two adjacent trimers in the helix especially by means of ion−ion, ion−dipole, and hydrogen bonding interactions. The interior of the helix has a rather large cavity, the boundaries of which are mainly fixed by O_{32} atoms, 6 Å away from the helical axis. Presumably, the cavity is filled by water molecules forming hydrogen bonds with the carboxylate groups, thus stabilizing the trimer. Other water molecules can form hydrogen bonds with the hydroxyl groups O_{25} and O_{26}. Of course, this model (Figure 2) can undergo slight changes without obtaining a remarkable worsening of the agreement between the observed and calculated data.

The present SAXS and DLS study was undertaken to investigate the NaGDC micellar size, shape, and structure in different conditions of interparticle interactions by extending both the ionic strength and the bile salt concentration range of the previous papers[1,3] in order to get more exhaustive information. The results concerning three series of aqueous solutions are presented: (1) 0.02 M NaGDC, 0−0.70 M NaCl (increment of 0.10 M); (2) 0.10 M NaGDC, 0−0.60 M NaCl (increment of 0.10 M); (3) 0.60 M NaCl, 0.02−0.10 M NaGDC (increment of 0.02 M). These series present the following features: (1) low bile salt concentration and progressive screening of the repulsive Coulombic interactions; (2) moderate bile salt concentration and progressive screening of the repulsive Coulombic interactions; (3) good screening of the repulsive Coulombic

interactions and a progressive increase of the bile salt concentration between the values of series 1 and 2.

The ambitious and main aim of this work is to determine with satisfactory approximation the NaGDC micellar aggregate structure at a gross molecular level. In the following, the experimental data will be treated assuming monodispersity for all the three series.

Experimental Section

Materials. NaGDC (Sigma, ≥97%) was crystallized in a mixture of water and acetone. Crystals were heated at 60 °C under a pressure of 10^{-2} torr for 1 day to remove water and acetone before preparing the aqueous electrolyte solutions. NaCl (Merck, suprapur) was used.

DLS Measurements. The Brookhaven instrument constituted by a BI-2030AT digital correlator with 136 channels and a BI-200SM goniometer was used. The light source was a Uniphase solid-state laser system model 4601 operating at 532 nm. Dust was eliminated by means of a Brookhaven ultrafiltration unit (BIUU1) for flow-through cells, the volume of the flow cell being about 1.0 cm^3. Nuclepore filters with a pore size of 0.1 μm were used. The samples were placed in the cell for at least 30 min prior the measurement to allow for thermal equilibration. Their temperature was kept constant within 0.5 °C by a circulating water bath. Measurements (laser power 50 mW) were repeated after 24 and 48 h to be sure that data were reproducible.

DLS measurements provided the field autocorrelation function $g_1(\tau)$ by means of the relation:[12,13]

$$g_2(\tau) = \frac{\langle I(t)I(t+\tau)\rangle}{\langle I(t)\rangle^2} = 1 + B{g_1}^2(\tau)$$

where $I(t)$ is the intensity at time t, $g_2(\tau)$ is the intensity autocorrelation function, and B is an instrument factor. The apparent diffusion coefficient D_a can be inferred from:

$$\ln g_1(\tau) = -q^2 D_a \tau + \frac{\mu_2 \tau^2}{2}$$

where q is the scattering vector and μ_2 is the so-called second cumulant.

The time-dependent light scattering correlation function was analyzed only at the 90° scattering angle. Apparent diffusion coefficients did not depend on the exchanged wave vector in the range 30−150° under our experimental conditions. Scattering decays were analyzed by means of cumulant expansion up to second order, because higher order contributions did not improve the statistics.

SAXS Measurements. SAXS experiments were performed on a Kratky compact system equipped with a NaI scintillation counter in a temperature-controlled room at 25 ± 1 °C and on the SAXS station at the Dutch−Belgian beamline (DUBBLE), BM26B, at the European Synchrotron Radiation Facility in Grenoble, France.[14] The data recorded on the Kratky camera were collected by using a quartz capillary of 1 mm, containing the NaGDC solution, and Ni-filtered Cu Kα radiation (λ = 1.5418 Å). Scattering curves were recorded within the range $0.012 \le k \le 0.5$ Å^{-1} ($k = 4\pi \sin\theta/\lambda$). The moving slit method was employed to measure the intensity of the primary beam.[15]

The collimated scattering intensities were put on an absolute scale and expressed in electrons^2/Å^3 (e.u.) per centimeter of primary beam length.[15,16] In terms of the total scattering cross section of an ensemble of particles, one e.u. corresponds to 7.94056×10^{-2} cm^{-1}.[17]

The data recorded on the BM26B were a quarter of the solid angle diffusion and were collected with a gas multiwire two-dimensional detector, (13 × 13) cm^2, with a pixel size of about 250 μm at a sample-to-detector distance of 3 m by using an X-ray wavelength of 1.24 Å (10 keV). The monochromatic incident light from the radiation spectrum of the source was obtained by using a double crystal Si (111) monochromator with saggital focusing on the second crystal to give an intense monochromatic X-ray beam in the range from 5 to 30 keV. The beam had fixed (0.3 × 0.3) mm^2 output slits and a transmission bandwidth of $\Delta\lambda/\lambda \sim 2 \times 10^{-3}$. Especially the NaGDC low concentration (0.02 M) samples benefit of the beam strong intensity that allows us to collect more reliable SAXS data. Thanks to the small size of the slits, the process of data desmearing could be neglected. Silver behenate was used as a low-angle diffraction standard to check the proper alignment and to calibrate the instrumentation.[18] The samples were filled in 2 mm diameter sealed Lindemann capillaries and kept in a thermostated sample holder at 25 °C. SAXS data were subsequently normalized to the intensity of the primary beam for absorption and for detector uniformity and were radially averaged. Experimental scattering curves were converted to absolute intensities expressed in eu by means of an elastomer standard with a known scattering intensity. The observed intensities were corrected for the contribution of the solvent-filled capillary under identical conditions.

If the particle interactions are neglected, the scattered intensities $I(k)$ depend on the form factor alone and can be expressed as

$$I(k) = \int_0^\infty p(r)\frac{\sin(kr)}{kr}\,dr$$

where $p(r)$, the electron pair distribution function, is related to the correlation function $\gamma(r)$[19,20] according to $p(r) = 4\pi\gamma(r)r^2$. The $p(r)$ function is strongly dependent on the shape and size of the scattering particles and vanishes at the maximum electron pair distance (D_M) within the particle. The effect of the interparticle interference can be frequently observed on the intensity and $p(r)$ curves at low NaCl concentrations. The $p(r)$ amplitude lowers with increasing distance, r, and goes to a negative minimum in the D_M region.[21]

Starting from the smeared or desmeared intensities, the indirect Fourier transform method developed in the ITP program allowed us to calculate the $p(r)$ function, the zero angle intensity I_0, and the electronic radius of gyration R_g.[22] When a molecular model of known geometry is assumed, the $I(k)$ and $p(r)$ functions can be calculated and compared with the observed ones. The calculations of $I(k)$, $p(r)$, and R_g corresponding to the 2_1 helix model were performed by a method proposed by Glatter, using the program MULTIBODY.[23] The effective charge of the atoms, Z_{eff}, was computed by means of the relationship $Z_{eff} = Z - V\rho_s$ where Z is the atomic number, ρ_s is the solvent electronic density, and V is the atomic van der Waals volume.[24]

The calculated intensities compared with those collected with the Kratky camera were smeared by the normalized weighting functions for slit length and slit width effects.[25] The best agreement with the experimental data was obtained by minimizing the function

$$R = \frac{1}{N}\sum_i \frac{(I_{o_i}(k) - I_{c_i}(k))^2}{{\sigma_i}^2}$$

TABLE 1: Some Relevant SAXS and DLS Experimental Data of the 0.02 M NaGDC Samples[m]

[NaCl]	N[a]	N^o[b]	R_g[c]	R_g*[d]	R_c[e]	h[f]	h^o[g]	h*[h]	D_M[i]	D_M*[j]	R_h[k]	R_h^{OG}[l]
0.10	27	28(2)	16.8(2)	16.2	11.5(5)	42(3)	41(6)	32	55(5)	56	15.9(1.0)	22.8
0.20	36	40(1)	18.0(2)	18.2	11.4(3)	48(2)	50(2)	43	60(5)	64	19.9(6)	24.0
0.30	42	42(1)	19.7(1)	19.7	13.2(2)	51(1)	48(2)	50	65(5)	70	22.6(5)	24.6
0.40	48	44(1)	21.1(1)	21.3	12.8(4)	58(2)	60(3)	58	75(10)	76	24.8(5)	25.9
0.50	54	59(2)	24.5(1)	22.9	14.3(8)	69(3)	69(5)	65	85(10)	80	28.1(6)	27.9
0.60	69	62(1)	26.2(3)	27.3	13.9(4)	77(2)	80(4)	83	92(10)	95	30.4(6)	29.3
0.70	90	94(6)	35.6(3)	33.9	13.6(1)	114(2)	117(8)	108	135(15)	118	34.5(4)	35.5

[a] Aggregation number from the observed and calculated intensity best fitting. [b] Aggregation number from ITP. [c] Observed radius of gyration (Guinier plot). [d] R_g of the 2_1 helical aggregate. [e] Observed radius of gyration of the cross section (Guinier plot). [f] Height of the helical aggregate from the relationship $h = [12(R_g^2 - R_c^2)]^{1/2}$. [g] Height of the helical aggregate from the zero angle intensity and the cross-section zero angle intensity. [h] Height of the 2_1 helical aggregate. [i] Observed maximum electron pair distance within the particles. [j] D_M of the 2_1 helical aggregate. [k] Observed apparent hydrodynamic radius. [l] R_h calculated by means of the method of Ortega and Garcia de la Torre.[31] [m] All the values are in angstroms, except those of the first three columns. Errors are in parentheses.

TABLE 2: Some Relevant SAXS and DLS Experimental Data of the 0.10 M NaGDC Samples[a]

[[NaCl]	N	N^o	R_g	R_g*	R_c	h	h^o	h*	D_M	D_M*	R_h	R_h^{OG}
0.20	30	31(3)	16.0(3)	17.1	13.5(3)	30(3)	28(2)	36	50(5)	60	18.6(3)	20.4
0.30	42	46(1)	19.7(3)	19.9	14.0(2)	48(2)	43(2)	50	68(5)	70	26.0(3)	24.0
0.40	54	57(3)	21.9(3)	23.2	13.0(1)	61(2)	63(4)	65	78(5)	80	31.9(3)	26.4
0.50	84	89(3)	32.1(4)	32.0	13.3(2)	101(2)	95(6)	101	115(10)	112	40.3(3)	33.3
0.60	117	113(5)	42.5(4)	42.6	13.4(2)	140(2)	146(4)	140	160(15)	148	52.6(3)	39.6

[a] The symbols have the same meaning as in Table 1. All the values are in angstroms, except those of the first three columns. Errors are in parentheses.

where $1 \le i \le N$ (number of experimental points), $I_{o_i}(k)$ and $I_{c_i}(k)$ are the observed and calculated intensities, and σ_i^2 is the $I_{o_i}(k)$ variance.

The distribution of the electron density contrast within the radial cross section of a cylinder can be calculated from the deconvolution of the $p(r)$ cross-section function. In our case, due to the limits of resolution in the real space, the modest diameter of the cross section does not guarantee a sufficient quality of the deconvolution. A quantitative estimate of the radial cross-section electronic density profile of the NaGDC aggregates was obtained by means of fitting the observed scattering intensities with scattering functions of cylinders with a three-shell cross section. The expression for the form factor of a cylinder with radius R and height L was given by Fournet:[26]

$$P(k) = \int_0^{\pi/2} \left[\frac{2B_1(kR \sin \alpha)}{kR \sin \alpha} \frac{\sin((kL \cos \alpha)/2)}{(kL \cos \alpha)/2} \right]^2 \sin \alpha \, d\alpha$$

where B_1 indicates the first-order Bessel function.

A generalized form factor for a cylinder consisting of N concentric shells with radii R_i and ρ_i electronic densities can be expressed as[27]

$$I(k) = \frac{1}{M} \sum_{i=1}^{N} (\rho_i - \rho_{i+1}) V_{R_i} P(k,R_i)$$

where ρ_{N+1} is the solvent electron density, V_{R_i} is the volume of the cylinder of radius R_i and height L, and M is the scattering mass of the particle given by

$$M = \sum_{i=1}^{N} (\rho_i - \rho_{i+1}) V_{R_i}$$

For a three-shell cylindrical model, seven parameters (the cylinder height h together with the radii R_i and the electronic densities ρ_i of the three shells) must be fitted to the scattering curves recorded in a finite k-range.

According to Shannon's sampling theorem, the number of free-fitting parameters, N_p, is restricted to $N_p \approx k_{max} D_M/\pi$ where k_{max} is the upper limit of the k-range with useful scattering data.[28,29] Under our conditions, the restriction on the maximum free parameter numbers is fulfilled. Moreover, the R_i and ρ_i parameters have been obtained by a simultaneous fitting of five experimental intensity curves with NaGDC or NaCl constant concentrations. The analytical NaGDC concentration was corrected by its critical micelle concentration at different NaCl concentrations.[30]

Experimental Results and Discussion

Low Bile Salt Concentration Series. The NaGDC low concentration reasonably ensures that weak attractive forces are present and even that the repulsive Coulombic ones are negligible at the highest ionic strengths. Thus, only the hard-body repulsion due to the excluded-volume effect of the micellar aggregates could be moderate or strong depending on their size. However, a simple calculation accomplished by assuming monodispersity and the cylindrical aggregate (aggregation number = 146 and cylindrical height = 175 Å) proposed for the 0.10 M NaGDC sample containing 0.70 M NaCl, previously investigated,[8] shows that for a 0.02 M NaGDC aqueous solution each aggregate has at its disposal a cubic box with an edge of about 230 Å, which is longer than the height (h) of the above-mentioned sample. Very probably, the samples of the low bile salt concentration series should have h and aggregation number values much lower, owing to their lower NaGDC and NaCl concentrations (see Table 1). Hence, the corresponding aggregates should give rise to a negligible excluded-volume effect and should be suitable to achieve structural information when the ionic strength is high.

Thus, it is reasonable to expect that the experimental data inferred from the SAXS spectra of this series do not suffer sensible interference effects and can be considered very reliable with the exception of those belonging to solutions at low NaCl concentrations, which can be affected by not negligible repulsive Coulombic interactions. Some SAXS and DLS data of the 0.02 M NaGDC series are given in Table 1, whereas those of series 2 and 3 are reported in Tables 2 and 3, respectively. They are the following:

TABLE 3: Best Fitting Cylinder Height *h* (Å) and Ionization Degree α of the 0.02 and 0.10 M NaGDC SAXS Spectra at Low NaCl Concentration[a]

[NaGDC]	[NaCl]	*h*	α	*h*[b]	α[b]
0.10	0	28(1)	0.30	37.2	0.322
0.02	0	19(1)	0.36		
0.02	0.05	20(1)	0.01		

[a] Errors are in parentheses. [b] From ref 3.

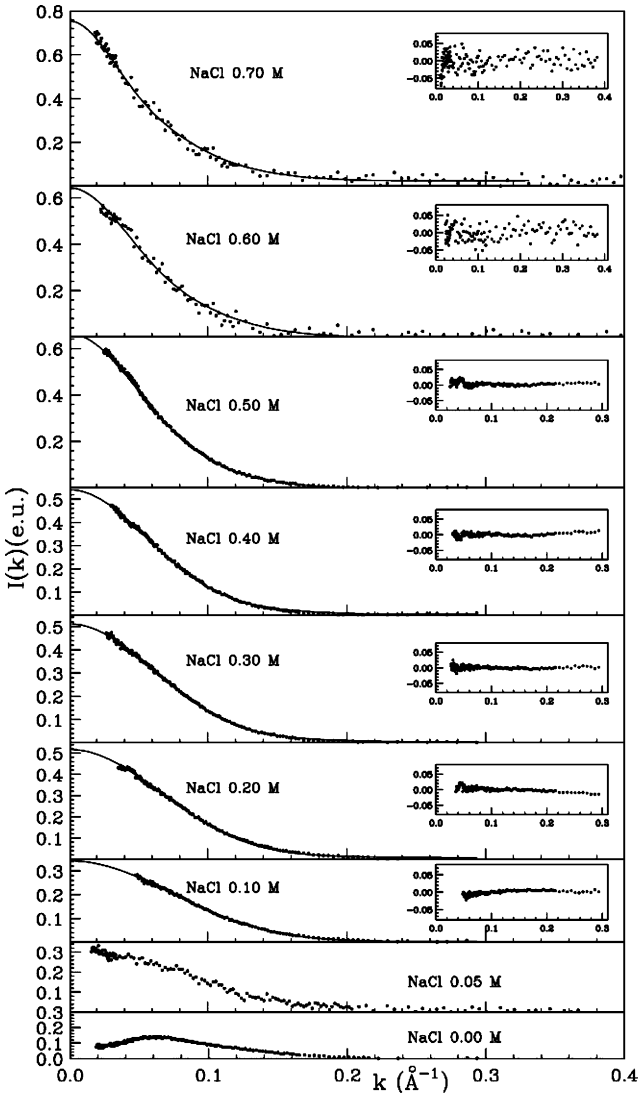

Figure 3. Experimental scattered intensities $I(k)$ of 0.02 M NaGDC aqueous solutions with NaCl concentrations within the range 0−0.70 M. The solid lines are calculated using, as a model, the 2_1 helix. The residuals are reported in the insets.

(i) the aggregation number (N) which gives the best fitting between the observed $I(k)$ and $p(r)$ functions and those calculated using, as a model, the 2_1 helix[23] (Figures 3 and 4). Only N values which were multiples of three were taken into account. The best fitting was obtained by tilting and shifting the NaGDC anion (having the geometry observed in the crystal[11]) with respect to the helical axis;

(ii) the aggregation number ($N°$) evaluated from ITP;

(iii) the observed radius of gyration (R_g) and radius of gyration of the cross section (R_c) calculated from the Guinier plots;

(iv) the height of the helical aggregate obtained from the relationships $h = [12(R_g^2 - R_c^2)]^{1/2}$ and $h^o = \pi I_0/I_c$, where I_0 and I_c are the zero angle intensity and the cross-section zero angle intensity, respectively, obtained by proper extrapolation at $k = 0$ accomplished on the experimental $I(k)$ function;

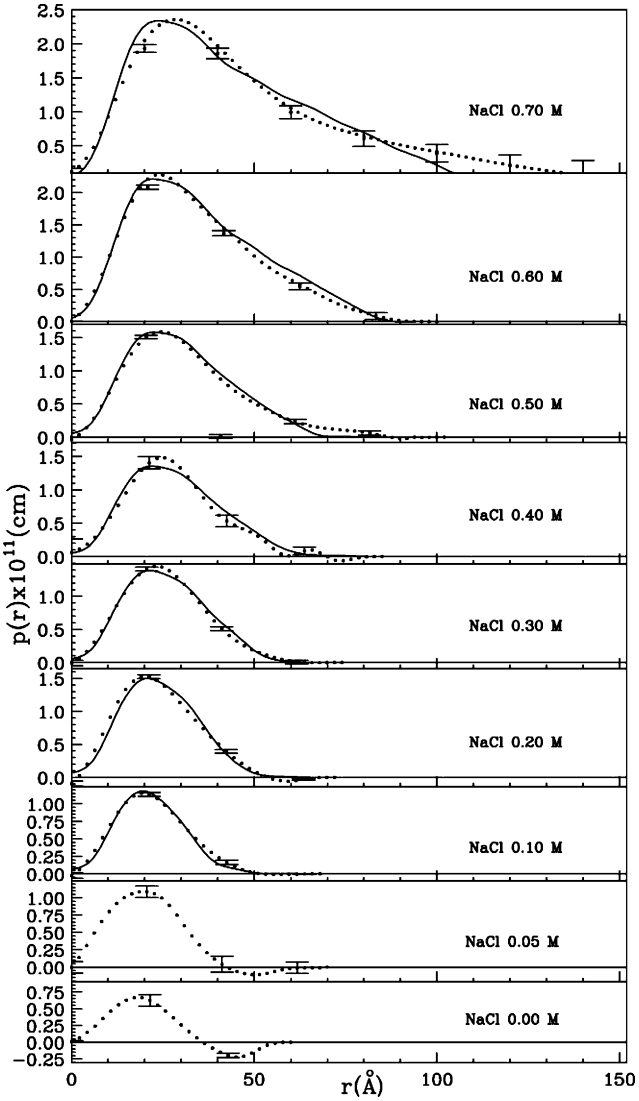

Figure 4. Experimentally derived $p(r)$ functions ($\times 10^{11}$ cm) of 0.02 M NaGDC aqueous solutions with NaCl concentrations within the range 0−0.70 M. The solid lines are $p(r)$ functions calculated using, as a model, the 2_1 helix. For clarity, only a few error bars of the observed $p(r)$ are shown.

(v) the maximum electron pair distance within the particles (D_M);

(vi) the observed apparent hydrodynamic radius (R_h) obtained from D_a by means of the Stokes−Einstein equation.

From the SAXS spectra, I_0, I_c, R_g, R_c, h, h^o, and D_M were determined. The starred symbols refer to the values calculated by using the 2_1 helical model ($t = 3.6$ Å). The R_g* and D_M* values were computed for the 2_1 helical aggregate with the proper N. The h* values were obtained from N because $h^* = (t/3)N = 1.2N$. The agreement between the observed and the 2_1 helical model calculated values is very satisfactory and strongly supports the proposed or a slightly modified model. In addition, it must be stressed that the SAXS technique permits a structural resolution at a gross molecular level and not at a finer atomic level.

The solutions without NaCl and with 0.05 M NaCl are not listed owing to a remarkable interference effect due to repulsive Coulombic interactions (see Figures 3 and 4). The effect of interactions will be discussed later on. The R_c average value of

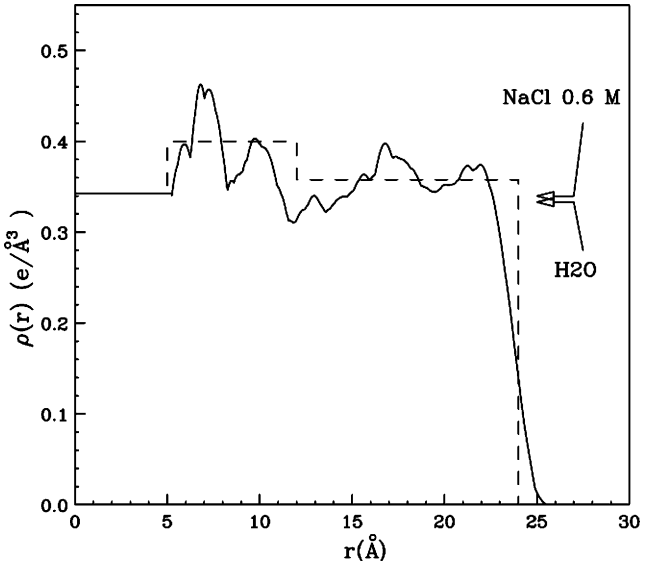

Figure 5. Calculated average radial electronic density $\rho(r)$ for the helical model with 48 water molecules (full line). The profile of the three-shell average radial electronic density used in the calculations is also shown (dashed line). The arrows indicate the NaCl 0.6 M and water electronic density.

13.5 Å for all the samples of the three series is in accordance with a micellar cylindrical shape.

To establish the solutions that are not affected by interference effects and provide the most reliable experimental data, observed R_h values were compared with those inferred from the SAXS structural parameters (R_h^{OG}).

The method of Ortega and Garcia de la Torre[31] for the description of the hydrodynamic properties of cylindrical (rodlike and discoidal) particles in dilute solution (noninteracting particles) was used.

In this method, which is valid for cylinders and disks with a length-to-diameter ratio (aspect ratio) ≥ 0.1,[31] the pertinent SAXS structural parameters (the average R_c and h values) of Tables 1, 2, and 3 were employed.

It must be stressed that the 2_1 helices of the 0.02 M NaGDC series are short enough so that their possible bending is inappreciable and, therefore, they can be regarded as straight and rigid cylindrical particles with low aspect ratio values less than 3 (see the h values of Table 1). The experimental R_h and the calculated R_h^{OG} values are compared in Table 1. They satisfactorily agree for the samples containing NaCl within the range 0.30−0.70 M, assuming a cylindrical diameter calculated from the expression $2R = 2\sqrt{2}R_c = 38.2$ Å, (if the R_c average value is used), valid for a cylinder with homogeneous electron density. This diameter is lower than the helical diameter ($2 \times 23.7 = 47.4$ Å). The shorter value is justified since the hydrodinamic properties of the helical structure cannot be rigorously reduced to those of a cylinder with the same size. On the contrary, the 0.10 and 0.20 M NaCl solutions seem to be affected by interference effects. Their R_c values are much lower than the average value of the other samples (13.5 Å), and also, their h and $h°$ values poorly agree with h^* (Table 1).

A rough estimate of the water molecule number per one NaGDC + $3H_2O$ unit can be performed supposing that the trimer volume is 6353 ($\pi \times 23.7^2 \times 3.6$) Å^3 and is completely filled by NaGDC and water molecules. Assuming molecular volumes of about 620 Å^3 for NaGDC, in accordance to calculated[24] and experimental[32] data, and 30 Å^3 for H_2O, about 50 water molecules per NaGDC molecule are evaluated (NaGDC:H_2O volume ratio of about 1:2.4), thus obtaining a high degree of hydration as in the case of NaTDC.[7,33] This number (about 50) is confirmed by filling all the space not occupied by NaGDC molecules with water molecules by means of the SOLVATE program[34] (48 molecules, Figure 2). The calculated average radial electronic density for the helical model with 48 water molecules together with a three-shell average radial electronic density indipendently evaluated on absolute scale are shown in Figure 5. The three-shell average radial electronic density leads to an R_c value of 13.5 Å in perfect agreement with the experimental average value. The two profiles shown in Figure 5 do not give significant differences in the calculations, thus supporting the helical model. As an example, the experimental scattering intensities and $p(r)$ functions of series 3 samples are compared with those calculated by means of a three-shell average radial electronic distribution (see Figures S1 and S2 in the Supporting Information). On the other hand, the aggregates are considerably inhomogeneous whether they are totally or partially filled by water, because the NaGDC molecular volume is less than one-third of the total, thus explaining the shortening of the cylindrical diameter.

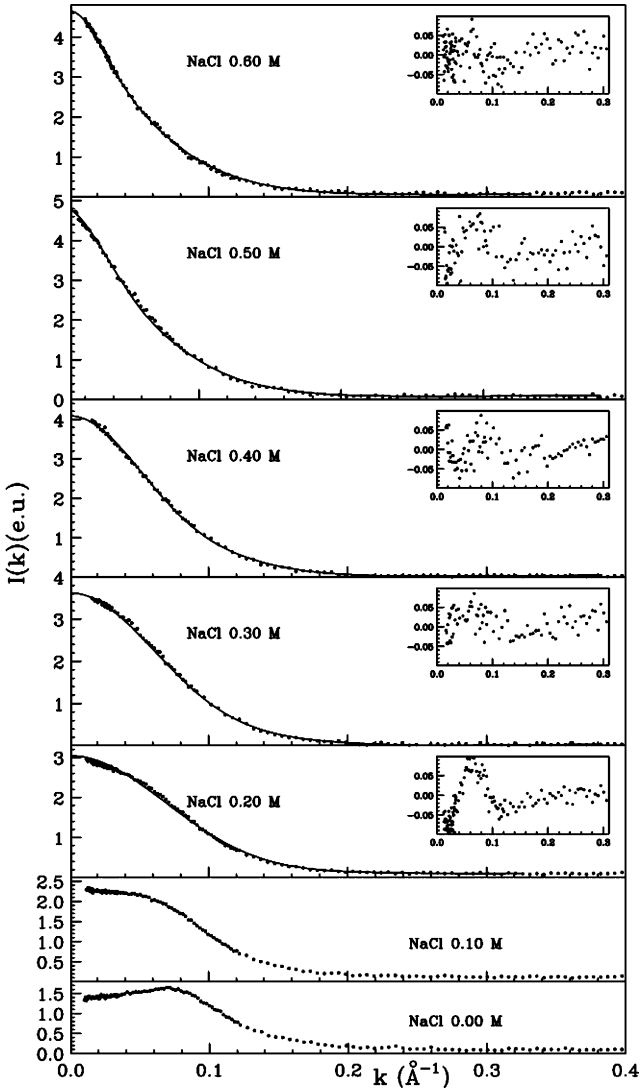

Figure 6. Observed smeared intensities $I(k)$ of 0.10 M NaGDC aqueous solutions with NaCl concentrations within the range 0−0.60 M. The solid lines are calculated using, as a model, the 2_1 helix. The residuals are reported in the insets.

In conclusion, the results indicate that the aggregates behave as small, noninteracting particles at the highest NaCl concentrations so that the experimental data inferred from the SAXS

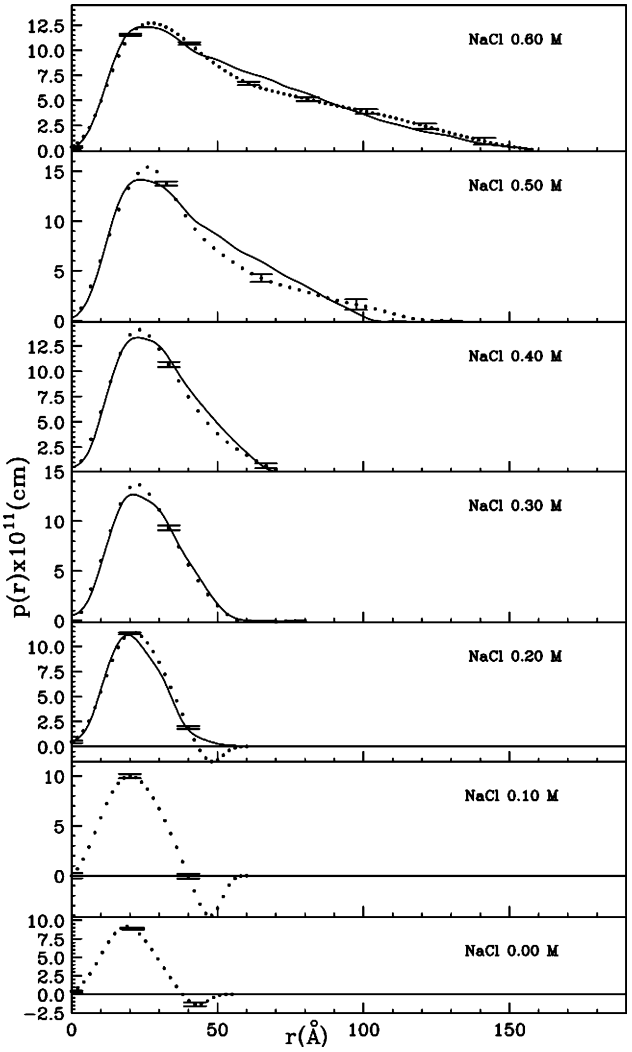

Figure 7. Experimentally derived $p(r)$ functions ($\times 10^{11}$ cm) of 0.10 M NaGDC aqueous solutions with NaCl concentrations within the range 0−0.60 M. The solid lines are $p(r)$ functions calculated using, as a model, the 2_1 helix. For clarity, only a few error bars of the observed $p(r)$ are shown.

spectra of the samples with NaCl within the range 0.30−0.70 M can be considered very reliable because they do not suffer sensible interference effects, as previously supposed. As expected, N, R_g, D_M, and R_h values show that the micellar size increases by increasing the NaCl concentration.

Moderate Bile Salt Concentration Series. The NaGDC moderate concentration (0.10 M) reasonably ensures that the repulsive Coulombic interactions are negligible at the highest ionic strengths. The hard-body repulsion due to the excluded-volume effect of the micellar aggregates can be roughly guessed by assuming monodispersity and the helical model. It has been inferred from the SAXS data that the 0.60 M NaCl sample (the sample with the biggest aggregate size) has an aggregation number of 117 (see Table 2). Each aggregate with $N = 117$ has at its disposal a cubic box with an edge of 126 Å, shorter than the h value of 140 Å calculated for this sample (see Table 2). Thus, interference effects due to hard-body repulsion, at least, are present.

The average R_c value is equal to 13.5 Å (see Table 2), thus supporting again a micellar cylindrical shape. On the other hand, the agreement between the observed and the 2_1 helical model calculated SAXS values of the samples with NaCl concentrations within the range 0.20−0.60 M is satisfactory, while the experimental R_h and the calculated R_h^{OG} values markedly differ.

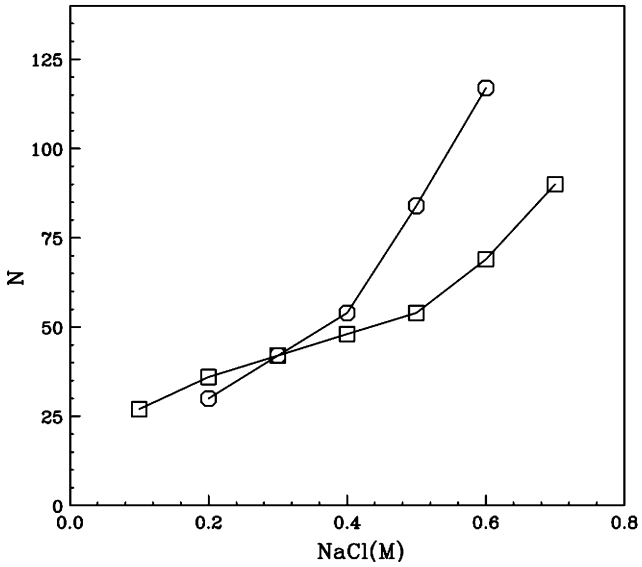

Figure 8. Aggregation number N vs NaCl concentration: (open squares) series 1; (open circles) series 2.

As for the low bile salt concentration series, the solutions at low NaCl molarities (≤0.1 M) are not listed owing to a remarkable interference effect due to repulsive Coulombic interactions (see Figures 6 and 7).

Previously, SAXS spectra of NaGDC solutions at low ionic strength were interpreted by accounting for the particle interaction effect (ref 3). In that case, a homogeneous cylinder was used to describe the micellar aggregates and the evolution of the particle size and interaction potential as a function of the added electrolyte concentration was analyzed. The effect of interactions on SAXS spectra was explored in terms of the decoupling approximation, and the method of Hayter and Penfold for a charged hard-sphere system was used to compute the interparticle structure factor ($S(k)$).[35] The same interaction model was used in this work to fit the spectra at low NaCl molarities of the low and moderate bile salt concentration series. By assuming three-shell cylindrical aggregates with fixed radii and electronic densities, the fits were carried out by varying the cylinder length h and the aggregate ionization degree α. The best fitting parameters for the solutions at NaCl ≤0.05 M are reported in Table 3 together with those of ref 3. The corresponding curves together with $S(k)$ are reported in the Supporting Information (Figure S3). In fact, when applied to higher NaCl concentrations, we observe that a remarkable lowering of α occurs and $\alpha = 0$ is obtained at NaCl ≥0.1 M. Since this value represents the minimum for the applicability of the method of Hayter and Penfold for charged particles, the results inferred for these samples are questionable and we did not report them. An inspection of Table 3 points out that the h and α values obtained in this work at 0.1 M NaGDC and no added salt are roughly similar to those of our previous paper. As a further result, we obtained that the α value slightly decreases by increasing the NaGDC concentration.

The aggregate growth seems to be approximately linear within narrow ranges of NaCl concentration for series 1 and 2. The aggregation number increases for an addition of NaCl 0.10 M by 6 or 15 within the range 0.20−0.50 or 0.50−0.70 M of NaCl, respectively, for series 1, and by 12 or 30 within the range 0.20−0.40 or 0.40−0.60 M of NaCl, respectively, for series 2

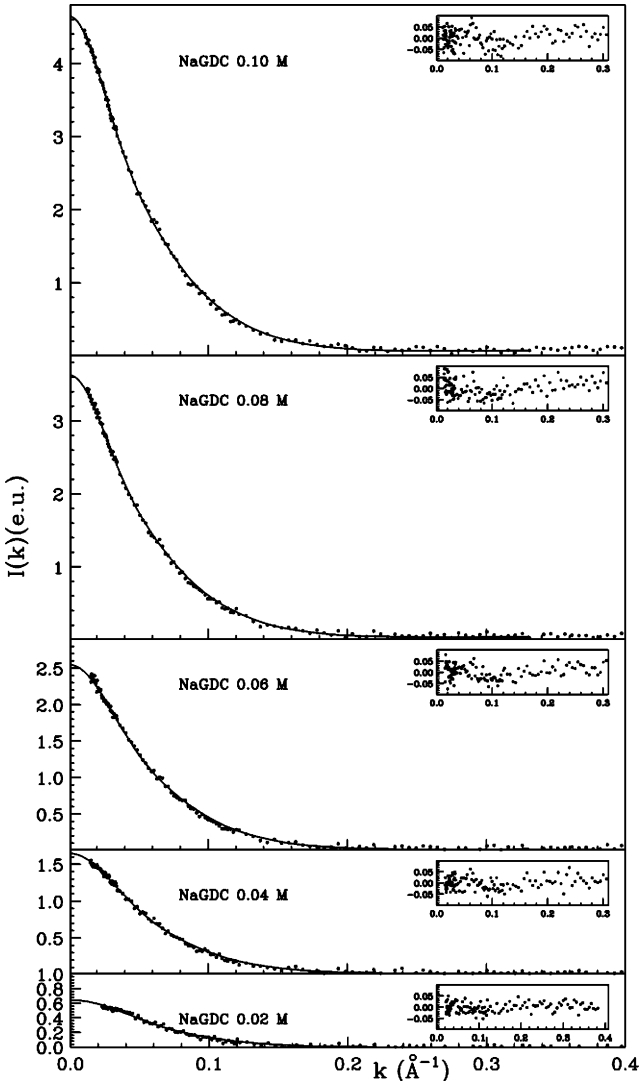

Figure 9. Observed smeared intensities $I(k)$ of aqueous solutions with NaGDC concentrations within the range 0.02−0.10 and 0.60 M NaCl. The solid lines are calculated using, as a model, the 2_1 helix. The residuals are reported in the insets.

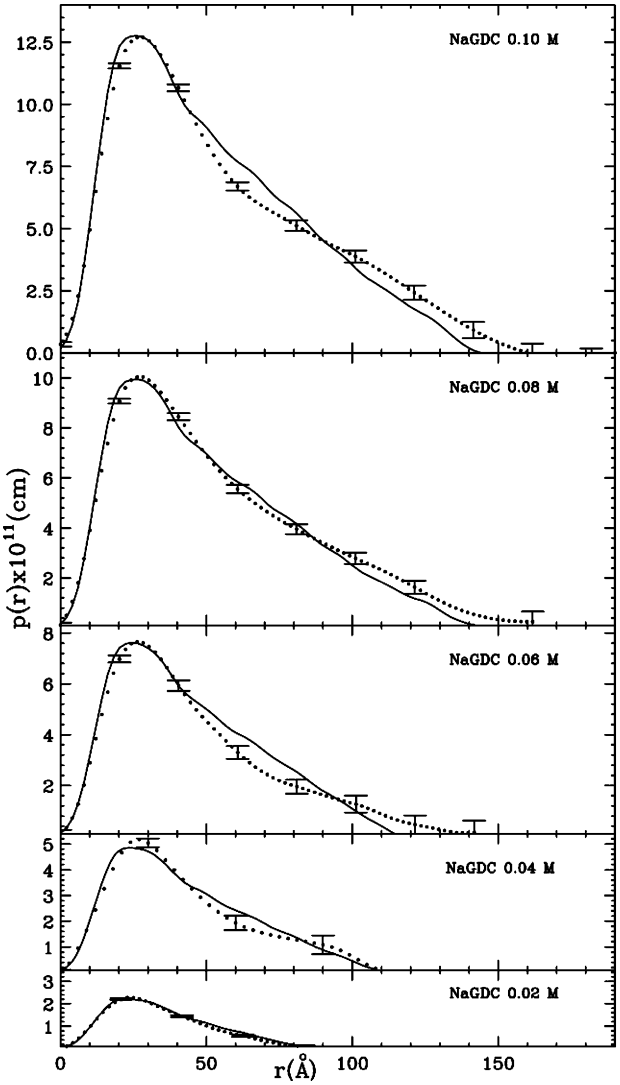

Figure 10. Experimentally derived $p(r)$ functions ($\times$ 10^{11} cm) of aqueous solutions with NaGDC concentrations within the range 0.02−0.10 and 0.60 M NaCl. The solid lines are $p(r)$ functions calculated using, as a model, the 2_1 helix. For clarity, only a few error bars of the observed $p(r)$ are shown.

(Figure 8). These results seem to indicate that the population of a certain species controls, within an ionic strength range, the aggregate growth, that occurs mainly by the addition of oligomers, formed by trimers. In this connection, it must be remembered that oligomers such as trimers, dodecamers, and pentadecamers, which are often present in the NaGDC and, chiefly, NaTDC aqueous electrolyte solutions,[9,10] could easily explain the above-mentioned aggregation number increase.

Progressive Increase of the Bile Salt Concentration at 0.6 M NaCl. The study of this series is useful to clarify the NaGDC concentration effects. The NaGDC concentrations and the high ionic strength of this series ensure that the repulsive Coulombic interactions are negligible more than in the case of series 2, with the exception of the 0.10 M NaGDC sample that is common to both series. The cylindrical aggregate shape is confirmed because the average R_c value is equal to 13.5 Å as in series 1 and 2. Interference effects occur due to hard-body repulsion, which increases by increasing the NaGDC concentration and the aggregate size (Table 3), and to attractive forces, which reasonably increase by increasing NaGDC concentration. Again, the agreement between the observed and the 2_1 helical model calculated SAXS values is satisfactory (Figures 9 and 10 and Table 4), while the experimental R_h and the calculated R_h^{OG} values markedly differ. Their difference increases by increasing the aggregate size, namely the NaGDC concentration in this series or the NaCl concentration in series 2. Because the experimental R_h is systematically greater than R_h^{OG}, the attractive term effect could prevail on the hard-body repulsive one in this series, because both the attractive and hard-body repulsive terms raise. A similar conclusion, even though the trend of the attractive term as a function of the micellar size is unknown, should be invoked for series 2. Since the SAXS data were interpreted by taking into account the $I(k)$ curves without the region at lowest k, which is the most influenced by interference effects, we believe that they allowed a reliable description of the helical structure.

Conclusions

SAXS and DLS measurements, accomplished on NaGDC aqueous electrolyte solutions at different conditions of interparticle interactions by varying the ionic strength (NaCl concentration from 0 to 0.70 M) and NaGDC concentration (from 0.02 to 0.10 M), permit us to establish that, assuming monodispersity, the NaGDC micellar aggregate structure at a

TABLE 4: Some Relevant SAXS and DLS Experimental Data of the 0.60 M NaCl samples[a]

[[NaGDC]	N	N^o	R_g	R_g*	R_c	h	h^o	h*	D_M	D_M*	R_h	R_h^{OG}
0.02	69	62(1)	26.2(3)	27.3	13.9(4)	77(2)	80(4)	83	92(10)	95	30.4(6)	29.3
0.04	90	84(3)	33.0(4)	33.9	12.8(5)	105(2)	112(7)	108	120(10)	118	36.0(1)	34.0
0.06	96	92(2)	36.0(5)	35.8	13.6(4)	116(2)	115(2)	115	140(10)	125	42.2(2)	35.8
0.08	114	111(4)	41.0(8)	41.7	13.6(2)	134(3)	144(7)	137	160(15)	145	47.3(2)	38.6
0.10	117	113(5)	42.5(4)	42.6	13.4(2)	140(2)	146(4)	140	160(15)	148	52.6(2)	39.6

[a] The symbols have the same meaning as in Table 1. All the values are in angstroms, except those of the first three columns. Errors are in parentheses.

gross molecular level can be described with satisfactory approximation by a 2_1 helix formed by trimers. The trimer is the repetitive unit and is constituted by three NaGDC and nine H_2O molecules related by a 3-fold rotation axis coinciding with the helical axis. SAXS data agree with the corresponding functions calculated using the 2_1 helix as model. This helix is described by a hollow cylinder with a conventional radius of 23.7 Å and a trimer repeat along the helical axis of 3.6 Å and is considerably inhomogeneous, since the NaGDC molecular volume in the cylinder is less than one-third of the total. On the other hand, the model is supported by calculations, without significant differences, performed with the average radial electronic density of the helix without water molecules or totally filled by water molecules (NaGDC/H_2O molecular ratio of about 1/50) or by using a three-shell average radial electronic density, independently evaluated on absolute scale.

Three series of aqueous solutions are investigated: (i) 0.02 M NaGDC, 0−0.70 M NaCl (increment of 0.10 M); (ii) 0.10 M NaGDC, 0−0.60 M NaCl (increment of 0.10 M); (iii) 0.60 M NaCl, 0.02−0.10 M NaGDC (increment of 0.02 M). The aggregate size increases for all the samples by increasing either the NaCl or NaGDC concentration. The NaGDC low concentration (0.02 M) samples with NaCl within the range 0.30−0.70 M are characterized by short cylindrical aggregates that do not give rise to sensible interference effects. The NaGDC moderate concentration (0.10 M) samples with NaCl within the range 0.20−0.60 M are characterized by cylindrical aggregates that, in the presence of progressively weaker repulsive Coulombic interactions, cause interference effects, due to the hard-body repulsion and attractive forces. The samples with a variable NaGDC concentration (0.02−0.10 M) at a fixed and high NaCl concentration (0.60 M) contain cylindrical aggregates that give rise to an attractive term effect prevailing on the hard-body repulsive one as well as for the NaGDC moderate concentration samples. However, the agreement between observed and calculated SAXS data is good for series 2 and 3 as well as for series 1. These results are supported by the comparison between the observed apparent mean hydrodynamic radii and the ones calculated by means of the method of Ortega and Garcia de la Torre,[31] valid for rods with a length-to-diameter ratio ≥ 0.1 in dilute solution (noninteracting rods). The results of the low and moderate NaGDC concentration samples seem to indicate that the increase of the aggregation number, produced by adding 0.10 M NaCl, is constant within an ionic strength range and occurs by the addition of oligomers formed by trimers.

Acknowledgment. This work was sponsored by Italian Ministero dell'Istruzione, dell'Università e della Ricerca. The authors would like to acknowledge the ESRF for the financial support (Proposal S.C.1233) and the Dutch−Belgian Beamline (DUBBLE) research group at the ESRF, France, for their help and support.

Supporting Information Available: NaGDC + $3H_2O$ atomic coordinates (Å) of the non-hydrogen atoms, used in building up the trimer and the cylindrical aggregates formed by trimers, given in a right-handed rectangular framework *OXYZ* with the *OZ*-axis coinciding with the 3-fold rotation axis of the trimers. The experimental scattering intensities and $p(r)$ functions of series 3 samples and those calculated by means of a three-shell average radial electronic distribution are shown in Figures S1 and S2. Moreover, the experimental and the calculated intensities (samples of Table 3) in the presence of interparticle interactions are shown in Figure S3. This material is available free of charge via the Internet at http://pubs.acs.org.

References and Notes

(1) Janich, M.; Lange, J.; Graener, H. *J. Phys. Chem. B* **1998**, *102*, 5957.
(2) Verwey, E. J. W.; Overbeek, J. T. G. In *Theory of the Stability of Lyophobic Colloids*; Elsevier: New York, 1948.
(3) Galantini, L.; Giglio, E.; Leonelli, A.; Pavel, N. V. *J. Phys. Chem. B* **2004**, *108*, 3078.
(4) Briganti, G.; D'Archivio, A. A.; Galantini, L.; Giglio, E. *Langmuir* **1996**, *12*, 1180.
(5) Galantini, L.; Giglio, E.; La Mesa, C.; Pavel, N. V.; Punzo, F. *Langmuir* **2002**, *18*, 2812.
(6) Bonincontro, A.; D'Archivio, A. A.; Galantini, L.; Giglio, E.; Punzo, F. *Langmuir* **2000**, *16*, 10436.
(7) Galantini, L.; Giglio, E.; Pavel, N. V.; Punzo, F. *Langmuir* **2003**, *19*, 1319.
(8) Galantini, L.; Giglio, E.; Pavel, N. V.; Punzo, F. *Colloids Surf. A* **2004**, *248*, 79.
(9) Bottari, E.; Festa, M. R. *Langmuir* **1996**, *12*, 1777.
(10) Bottari, E.; Festa, M. R. *Monatsh. Chem.* **1993**, *124* (11−12), 1119.
(11) Campanelli, A. R.; Candeloro De Sanctis, S.; Galantini, L.; Giglio, E. *J. Inclusion Phenom. Mol. Recognit. Chem.* **1991**, *10*, 367.
(12) Koppel, D. E. *J. Chem. Phys.* **1972**, *57*, 4814.
(13) Siegert, A. J. F. *On the fluctuations in signals returned by many independent, moving scatterers*; Report No 465, MIT (Mass. Inst. Technol.) Radiation Lab., 1943; pp 1−14.
(14) Bras, W. *J. Macromol. Sci., Phys.* **1998**, *B37*, 557.
(15) Stabinger, H.; Kratky, O. *Makromol. Chem.* **1978**, *179*, 1655.
(16) Glatter, O. In *Small Angle X-ray Scattering*; Glatter, O., Kratky, O., Eds.; Academic Press: London, 1982; p 119.
(17) Orthaber, D.; Bergmann, A.; Glatter, O. *J. Appl. Crystallogr.* **2000**, *33*, 218.
(18) Blanton, T. N.; Huang, T. C.; Toraya, H.; Hubbard, C. R.; Robie, S. B.; Louer, D.; Goebel, H. E.; Will, G.; Raftery, T. *Powder Diffr.* **1995**, *10*, 91.
(19) Porod, G. *Kolloid Z.* **1951**, *124*, 83.
(20) Debye, P.; Bueche, A. M. *J. Appl. Phys.* **1949**, *20*, 518.
(21) Glatter, O. In *Small Angle X-ray Scattering*; Glatter, O., Kratky, O., Eds.; Academic Press: London, 1982; p 167.
(22) Glatter, O. *J. Appl. Crystallogr.* **1977**, *10*, 415.
(23) Glatter, O. *Acta Phys. Austriaca* **1980**, *52*, 243.
(24) Durchschlag, H.; Zipper, P. *J. Com. Esp. Deterg.* **1995**, *26*, 275.
(25) Glatter, O. *J. Appl. Crystallogr.* **1974**, *7*, 147.
(26) Fournet, G. *Bull. Soc. Fr. Minéral. Crist.* **1951**, *74*, 39.
(27) Pedersen, J. S. *Adv. Colloid Interface Sci.* **1997**, *70*, 171.
(28) Shannon, C. E.; Weaver, W. In *The Mathematical Theory of Communication*; University of Illinois Press: Urbana, IL, 1949.
(29) Glatter, O. *J. Appl. Crystallogr.* **1980**, *13*, 577.
(30) Matsuoka, K.; Masato, M.; Yoshikiyo, M. *Colloids Surf., B* **2003**, *32*, 87.
(31) Ortega, A.; Garcia de la Torre, J. *J. Chem. Phys.* **2003**, *119*, 9914.
(32) Steele, J. C. H., Jr.; Tanford, C.; Reynolds, J. A. *Methods Enzymol.* **1978**, *48*, 11.
(33) Laurent, T. C.; Persson, H. *Biochim. Biophys. Acta* **1965**, *106*, 616.
(34) Grubmüller, H.; Heymann, B.; Tavan, P. *Science* **1996**, *271*, 997.
(35) Hayter, J. B.; Penfold, J. *Mol. Phys.* **1981**, *42*, 109.